

# Dynamic modelling of lettuce transpiration for water status monitoring

by Adeyemi, O., Grove, I., Peets, S., Domun, Y. and Norton, T.

**Copyright, Publisher and Additional Information:** This is the author accepted manuscript. The final published version (version of record) is available online via Elsevier.

This version is made available under the CC-BY-ND-NC licence:  
<https://creativecommons.org/licenses/by-nc-nd/4.0/legalcode>

Please refer to any applicable terms of use of the publisher

DOI: <https://doi.org/10.1016/j.compag.2018.10.008>





31 **Abstract**

32 Real-time information on the plant water status is an important prerequisite for the precision  
33 irrigation management of crops. The plant transpiration has been shown to provide a good  
34 indication of its water status. In this paper, a novel plant water status monitoring framework  
35 based on the transpiration dynamics of greenhouse grown lettuce plants is presented.  
36 Experimental results indicated that lettuce plants experiencing adequate water supply  
37 transpired at a higher rate compared to plants experiencing a shortage in water supply. A  
38 data-driven model for predicting the transpiration dynamics of the plants was developed  
39 using a system identification approach. Results indicated that a second order discrete-time  
40 transfer function model with incoming radiation, vapour pressure deficit, and leaf area index  
41 as inputs sufficiently explained the dynamics with an average coefficient of determination of  
42  $R_T^2 = 0.93 \pm 0.04$ . The parameters of the model were updated online and then applied in  
43 predicting the transpiration dynamics of the plants in real-time. The model predicted  
44 dynamics closely matched the measured values when the plants were in a predefined water  
45 status state. The reverse was the case when there was a significant change in the water  
46 status state. The information contained in the model residuals (measured transpiration –  
47 model predicted transpiration) was then exploited as a means of inferring the plant water  
48 status. This framework provides a simple and intuitive means of monitoring the plant water  
49 status in real-time while achieving a sensitivity similar to that of stomatal conductance  
50 measurements. It can be applied in regulating the water deficit of greenhouse grown crops,  
51 with specific advantages over other available techniques.

52 **Keywords:** Plant water status; Transpiration; Modelling; System Identification; Irrigation

53

54

55

56

57 **1 Introduction**

58 The precise determination of irrigation water requirement and timing is a precursor to the  
59 successful precision irrigation management of crops (Kochler et al., 2007). This requires a  
60 knowledge of the plant water status in real-time which can then guide in arriving at optimal  
61 irrigation scheduling decisions.

62 Contact monitoring methods such as measurements of stomatal conductance, sap-flow, and  
63 leaf turgor pressure have been shown to provide an adequate indication of plant water  
64 status. However, these methods are plant-based, requiring large replication to provide an  
65 indication of water status at crop level. They also require technical expertise for  
66 implementation, laborious and difficult to deploy as a real-time monitoring tool (Jones, 2004).

67 Non-contact measurement of plant canopy temperature ( $T_c$ ) which is normalized using a  
68 crop water stress index (CWSI) also provides a good indication of plant water status (Ben-  
69 Gal et al., 2009). Its application as a monitoring tool in commercial crop production is  
70 however limited because of the need to know the baseline temperatures which are required  
71 for its computation under the same environmental conditions as  $T_c$  (Maes and Steppe,  
72 2012). Non-contact monitoring tools which can provide a real-time indication of the plant  
73 water status at crop level, with non- laborious implementation, and minimal instrumentation  
74 and computation requirements will therefore be beneficial in implementing precision  
75 irrigation management in commercial crop production (Adeyemi et al., 2017).

76 The plant transpiration is perhaps the best indication of plant water status (Jones, 2008;  
77 Maes and Steppe, 2012). Plants experiencing unrestricted water supply (well-watered  
78 plants) have been shown to transpire at a higher rate when compared to plants experiencing  
79 a shortage in water supply (Ben-Gal et al., 2010; Villarreal-Guerrero et al., 2012). This is due  
80 to the regulation of water loss by the plant's stomates with the stomates of well-watered  
81 plants opening up more in response to atmospheric demand. The stomates of plants  
82 experiencing water shortage open up less in response to atmospheric demand in order to

83 limit water loss (Blonquist et al., 2009). Therefore, the water status of a plant can be inferred  
84 from measurements of its transpiration rate.

85 Traditionally, the knowledge of crop transpiration over time has been applied in the dynamic  
86 control of water supply to greenhouse crops (Daniel et al., 2013). This is usually in form of  
87 an off/off control strategy in which irrigation is applied after the accumulation of a set point  
88 cumulative transpiration amount (Davis and Dukes, 2010). These computer-controlled  
89 irrigation systems make use of mechanistic or empirical models to estimate crop  
90 transpiration based on environmental and physiological factors (Barnard and Bauerle, 2015).

91 Several models have been developed for the estimation of transpiration from greenhouse  
92 cultivated ornamental and vegetable crops (Baptista et al., 2005; Fatnassi et al., 2004; Jolliet  
93 and Bailey, 1992; Montero et al., 2001). Most of these models are based on the thermal  
94 energy balance equation of the plant canopy and are similar to the Penman-Monteith (PM)  
95 equation (Howell and Evett, 2004). These models are able to account for the effect of actual  
96 water supply on transpiration through the incorporation of a stomatal resistance component.  
97 The stomatal resistance is expressed as a function of several factors including solar  
98 radiation, leaf vapour pressure deficit, leaf temperature,  $CO_2$  concentration,  
99 photosynthetically active radiation, leaf water potential etc. (Kochler et al., 2007). The  
100 development of these models requires the calibration of several hard-to-measure  
101 parameters which limit their practical application as an irrigation monitoring tool (Villarreal-  
102 Guerrero et al., 2012). Furthermore, these models are unable to account for the time varying  
103 nature of the plant system, as their parameters are assumed to remain constant once  
104 identified. The response of a plant will vary as a result of growth, biotic and abiotic factors,  
105 and adaptation processes (Boonen et al., 2000).

106 Data-driven modelling approaches based on measured input-output data of a process have  
107 been shown to provide robust approximations of various biological processes and often  
108 require fewer input parameters when compared to mechanistic models (Navarro-Hellín et al.,  
109 2016). The later is difficult to implement as a perfect knowledge of the physical process

110 under consideration is often required (Bennis et al., 2008). Sánchez et al. (2012) applied a  
111 system identification approach in predicting the transpiration rate of a greenhouse grown  
112 tomato crop. Their approach showed promise in accounting to the time-varying plant  
113 response through an online update of the model parameters. Speetjens et al. (2009) also  
114 applied an extended Kalman filtering algorithm for the online estimation of model parameters  
115 for predicting the transpiration of a greenhouse grown crop. Both studies reported improved  
116 prediction of plant transpiration rates when compared to values predicted by mechanistic  
117 models. The modelling approach presented in both studies are data-driven making their  
118 practical application as an irrigation monitoring tool viable. They also do not require the  
119 stomatal behaviour to be modelled explicitly as it is accounted for in the online parameter  
120 estimation process.

121 System identification is a data-driven modelling approach which is applied in modelling  
122 dynamic systems (Chen and Chang, 2008). It has been successfully applied in simplifying  
123 and modelling complex environmental and biological processes (Taylor et al., 2007; Young,  
124 2006), predicting time-varying biological responses (Kirchsteiger et al., 2011; Quanten et al.,  
125 2006) and in many other irrigation decision support applications (Delgoda et al., 2016;  
126 Lozoya et al., 2016). It is extensively applied as part of the fault detection methodologies in  
127 the advanced process control industry (Young, 2006). During fault detection, a system  
128 identification approach is used to build a dynamic model of a process in a known healthy  
129 state. The output predicted by the model can then be compared to the actual real-time  
130 measurements from the process. The parameters of the model can also be updated as new  
131 data is acquired from the process (Gil et al., 2015). This methodology, which has proven to  
132 be successful in the process control industry, can be adapted and applied as part of an  
133 adaptive decision support system for irrigation monitoring (Adeyemi et al., 2017).

134 The objectives of this study are to investigate if the transpiration rates of greenhouse grown  
135 lettuce plants (*Lactuca sativa*) maintained at different water deficit levels will differ. This will  
136 provide a justification for the application of this measurement as a plant water status

137 monitoring tool. A system identification approach is thereafter applied in developing a model  
138 of the transpiration dynamics and predicting the transpiration rate of these plants. Finally, the  
139 predicted transpiration rate is used as a tool for monitoring the water status of the lettuce  
140 plants and real-time detection of deviations from a defined water status state.

## 141 **2 Background**

### 142 **2.1 Plant transpiration**

143 Plant transpiration can be described by the Penman-Monteith equation (Monteith, 1973).  
144 This equation and other transpiration models derived from it specify that the transpiration  
145 ( $T_p$  ( $gm^{-2}min^{-1}$ )) is dependent on the incoming solar radiation ( $R_{sw}$  ( $Wm^{-2}$ )) and the vapour  
146 pressure deficit of the ambient air ( $\Delta$  ( $kPa$ )). This is expressed as

$$147 \quad T_p = R_{sw}C_A + \Delta C_B \quad (1)$$

148 Where the coefficients  $C_A$  and  $C_B$  are crop dependent parameters.

149 Baille et al. (1994) noted that the coefficient  $C_B$  is a function of the plant leaf area index (LAI),  
150 and it adopts different values during the day due to oscillations in stomatal resistance.

### 151 **2.2 System identification**

152 System identification is applied in constructing mathematical models of dynamic systems  
153 based on the incoming time-series of input ( $u(t)$ ) and output ( $y(t)$ ) data. The goal is to infer  
154 the relationship between the sampled input/output data. During system identification, the  
155 model structure is first identified using objective methods of time series analysis based on a  
156 given general class of time-series models (here, linear discrete time transfer functions). The  
157 resulting model must be able to explain the structure of the observed data. System  
158 identification is used to simultaneously linearize and reduce model complexity, so exposing  
159 its 'dominant modes' of dynamic behaviour.

160 In this study, the identification process was conducted based on prior knowledge of the plant  
161 transpiration process as shown in equation 1. The vapour pressure deficit and incoming

162 radiation were selected as climatic input, and the LAI was selected as crop growth input. The  
 163 identification of the model structure is considered the first step of the identification problem in  
 164 the present study. An online estimation algorithm is thereafter implemented to update the  
 165 model parameters based on the real-time data obtained from the process.

166 In this way, it is possible to detect the changes in the dynamics of the system thus  
 167 accounting for the time-varying nature of the plant system.

168 The linear discrete-time transfer function is written as

$$169 \quad y(t) = \frac{B_1(L)}{A(L)} U_1(t - \delta_1) + \dots + \frac{B_k(L)}{A(L)} U_k(t - \delta_k) + e(t); e \sim WN(0, \sigma_e^2) \quad (2)$$

170 Where  $y(t)$  is the output (transpiration rate),  $U_i(t)$  ( $i = 1, 2, \dots, K$ ) are a set of  $K$  inputs that  
 171 affect the output (incoming radiation, vapour pressure deficit),  $\delta_i$  ( $i = 1, 2, \dots, K$ ) are the  
 172 delays associated with each input.

173 In equation 2,

$$174 \quad A(L) = 1 + a_1L + \dots + a_nL^n \quad (3)$$

$$175 \quad B(L) = b_0 + b_1L + \dots + b_mL^m$$

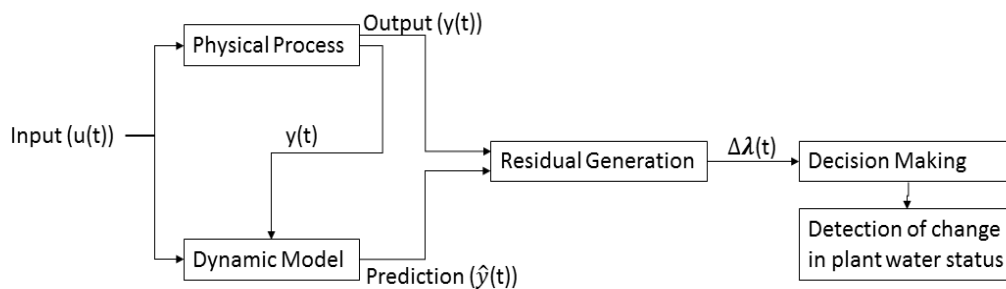
176  $A(L)$  and  $B(L)$  are polynomials of the order  $n$  and  $m$  respectively. The backshift operator  $L$  is  
 177 such that  $L^j y_t = y_{t-j}$ .  $a_i$  ( $i = 1, 2, \dots, n$ ) and  $b_j$  ( $j = 1, 2, \dots, m$ ) are coefficients of the  
 178 polynomials  $A(L)$  and  $B(L)$ . They represent the unknown parameters that are to be  
 179 identified. The identified model is defined by the triad  $[n, m_i, \delta_i]$ , where  $n$  is the number of  
 180 denominator parameters; indicating the model order, and  $m_i$  is the number of numerator  
 181 parameters associated with each input.  $\delta_i$  is defined earlier.

182 The identification process was conducted using the refined instrumental variable algorithm  
 183 (Taylor et al., 2007) implemented in the Captain toolbox (Young et al., 2007) on the  
 184 MATLAB® software.

185

186 **2.3 Plant water status monitoring framework**

187 The plant water status monitoring algorithm proposed in this paper is data-driven. The  
 188 algorithm is founded on an estimated dynamic model of the plant transpiration. The model is  
 189 identified as a time domain model and the parameters of the model are identified online from  
 190 the real-time measurements of input-output data. The water status monitoring principle is  
 191 based on a premise that the transpiration dynamics of a plant will vary as a function of the  
 192 prevailing climatic conditions and its water status. A model of the plant is built at a known  
 193 water status state and predictions from this model is then compared to real-time output data  
 194 obtained from the plant. A schematic illustration of the algorithm is presented in Figure 1.



195

196 Figure 1: Schematic illustration of the proposed water status monitoring framework

197 The decision-making module assumes that the residuals (measured transpiration – model  
 198 predicted transpiration) generated from a healthy mode of the process i.e. non-significant  
 199 deviation in water status state will conform to an established statistical distribution. A change  
 200 in this distribution will indicate a significant deviation in the water status state of the plant.

201 When there is a significant change in plant water status, the model obtained during a  
202 particular water status state is unable to predict the observed plant response. This causes  
203 the difference between the measured and predicted transpiration rate i.e. the magnitude of  
204 the residuals to increase. The decision-making algorithm is further explained in section 2.3.1

### 205 **2.3.1 Decision-making algorithm**

206 During system identification, the residuals obtained between the measured and modelled  
207 output is assumed to be a normally distributed Gaussian sequence (Taylor et al., 2007). For  
208 a properly defined model identified during a known process state, the residuals obtained  
209 between the measured and predicted output will also conform to this distribution. However,  
210 when there is a significant change in the process state, the distribution of the residuals  
211 obtained as a function of the predicted output will deviate from the distribution obtained  
212 during the modelling phase.

213 A Gaussian Mixture Model (GMM) can be applied in modelling the distribution of the  
214 residuals obtained during the identification process. The GMM assumes we have  $k$  normal  
215 distributions to describe the data  $\{N(\mu_1, \sigma_1) \dots \dots N(\mu_k, \sigma_k)\}$  and estimates the parameters for  
216 those individual distributions that when combined best describes the data (Reynolds, 2015).  
217 The probability of observing a value  $X_n^j$  for a specific data point is expressed as (Reynolds,  
218 2015)

$$219 \quad p(X_n^j) = \sum_{k=1}^k \pi_k \mathfrak{N}(X_n^j | \mu_k, \sigma_k) \quad (4)$$

220 With

$$221 \quad \sum_{k=1}^k \pi_k = 1$$

$$222 \quad \forall_k: 0 \leq \pi_k \leq 1$$

223 Where  $\mu_k$  and  $\sigma_k$  are the mean and standard deviations of each  $k$  distribution and  $\pi_k$   
224 expresses the weight of each distribution.

225 An expectation maximization algorithm is applied in deriving the parameters that maximize  
226 the likelihood of the GMM given the training data, here, the residuals obtained during  
227 identification. These parameters are then applied in computing the probability of each  
228 observation. The best number of distributions to fit the data is also determined by minimizing  
229 the Akaike information criterion (AIC) (Xiao et al., 2016).

230 Once the GMM is fitted on the training data, a normal or anomalous process state can be  
231 identified by computing the probability of observing the residuals computed for that state  
232 using the GMM fitted on the residuals obtained during identification. The probabilities of  
233 observing the residuals during the anomalous state will be much lower compared to the  
234 probability of observing the residuals obtained during the normal process state and also  
235 during identification. This methodology has been shown to achieve state of the art  
236 performance when detecting faults in rotary machinery and high-voltage electronic  
237 equipment (Yan et al., 2017).

238

### 239 **3 Materials and Methods**

#### 240 ***3.1 Greenhouse and experimental setup***

241 Two six week studies were conducted in a climate controlled greenhouse. The heating and  
242 ventilation set points were approximately 17 and 23°C respectively. Lettuce plants were  
243 planted in individual 2.5 L containers containing a sandy loam soil ( $FC= 0.186 m^3m^{-3}$  ,  
244  $PWP= 0.071 m^3m^{-3}$ ). To prevent evaporation, the soil surface of the pots were covered with  
245 a 5 cm layer of plastic beads.

246 During the initial study, the plants were irrigated every two hours. However, four hours prior  
247 to the initiation of measurements, four lettuce plants were selected and irrigated to replace  
248 100% of the water lost by transpiration, four plants were irrigated to replace 90% of the water  
249 lost by transpiration, and four other plants were irrigated to replace 75% of water lost by  
250 transpiration. These irrigation treatments are hereafter referred to as 100ET, 90ET and 75ET

251 respectively. Irrigation volumes corresponding to the treatments was applied every two  
252 hours. This approach was used in other to ensure the uniform development of the plant  
253 population's leaf area index.

254 During a follow-up study, after four hours into a diurnal measurement period, irrigation was  
255 withheld from four lettuce plants which have been receiving the 100ET irrigation treatment.  
256 Four other lettuce plants also received the 100ET irrigation treatment all through the diurnal  
257 measurement period. Irrigation was applied every two hours to these set of plants.

### 258 **3.2 Microclimate measurements**

259 Environmental variables measured at plant canopy level included ambient air temperature  
260 and relative humidity using a temperature and humidity probe (Model EE08, E+E Elektronik,  
261 Engerwitzdorf, Austria), and incoming radiation using a pyranometer sensor (Model SP-110,  
262 Apogee Instruments, Logan, Utah, USA). Wind speed was measured using a hot wire  
263 anemometer (Model AM – 4202, Lutron Electronics, London, UK) installed 10cm above the  
264 crop canopy. The VPD was calculated using temperature and relative humidity data  
265 following the equations outlined in Allen et al. (1998). Sensor readings were obtained at a 5  
266 s interval and averaged online over 1 min periods with a CR1000 data acquisition system  
267 (Campbell Scientific, Logan, Utah, USA). All sensors were factory calibrated by their  
268 respective manufacturers.

### 269 **3.3 Transpiration measurements**

270 Crop transpiration of the lettuce plants was measured using three load balance systems  
271 (Model ALC, Acculab, Englewood, USA) with a 16 kg capacity and  $\pm 0.1$  g resolution. Each  
272 load balance recorded the mass of the four plants in each treatment group.

273 The total transpiration for a time period was calculated as the mass difference,  $\Delta M$  between  
274 two consecutive time instants as recorded by the mass balance system. This was then  
275 converted to the units of volume by multiplying  $\Delta M$  by the density of water ( $1000 \text{ kgm}^{-3}$ ). In  
276 the various irrigation treatments, a computer controlled irrigation system applied irrigation to

277 replace the predefined percentage of water loss based on the calculated water loss volume.  
278 The total irrigation volume calculated for a treatment group was divided equally among the  
279 plants assigned to that group.

280 The transpiration rate was calculated as

$$281 \quad T_p = \frac{M(t_{i+1}) - M(t_i) j}{A \cdot (t_{i+1} - t_i) n} \quad (5)$$

282 Where  $M(t_i)$  is the mass ( $g$ ) given by the balance at time  $t_i$  ( $min$ ),  $A$  ( $m^2$ ) is the area of the  
283 shelf on which the plants are placed,  $n$  is the number of pots on the balance tray and  $j$  is  
284 the number of plants on the shelf. During irrigation, the transpiration rate was assumed to  
285 be constant. Data from the balance system was directly stored every minute.

#### 286 **3.4 Leaf area index measurements**

287 The leaf area index (LAI) values for the plants placed on the balance were assessed using  
288 digital images captured with a mobile phone camera. The LAI values were then extracted  
289 from the digital images using the Easy leaf area software (Department of Plant Sciences,  
290 University of California).

#### 291 **3.5 Ancillary measurements**

292 The soil moisture status of the plants placed on the balance was measured at hourly  
293 intervals using a model GS1 soil moisture sensor (Decagon Devices, Pullman, Washington,  
294 USA). The stomatal conductance of the plants was also measured using a diffusion leaf  
295 porometer (Model AP4, Delta-T Devices, Cambridge, UK) between 13:00 and 15:00 hrs local  
296 standard time.

297

298

299

## 300 **4 Results and discussion**

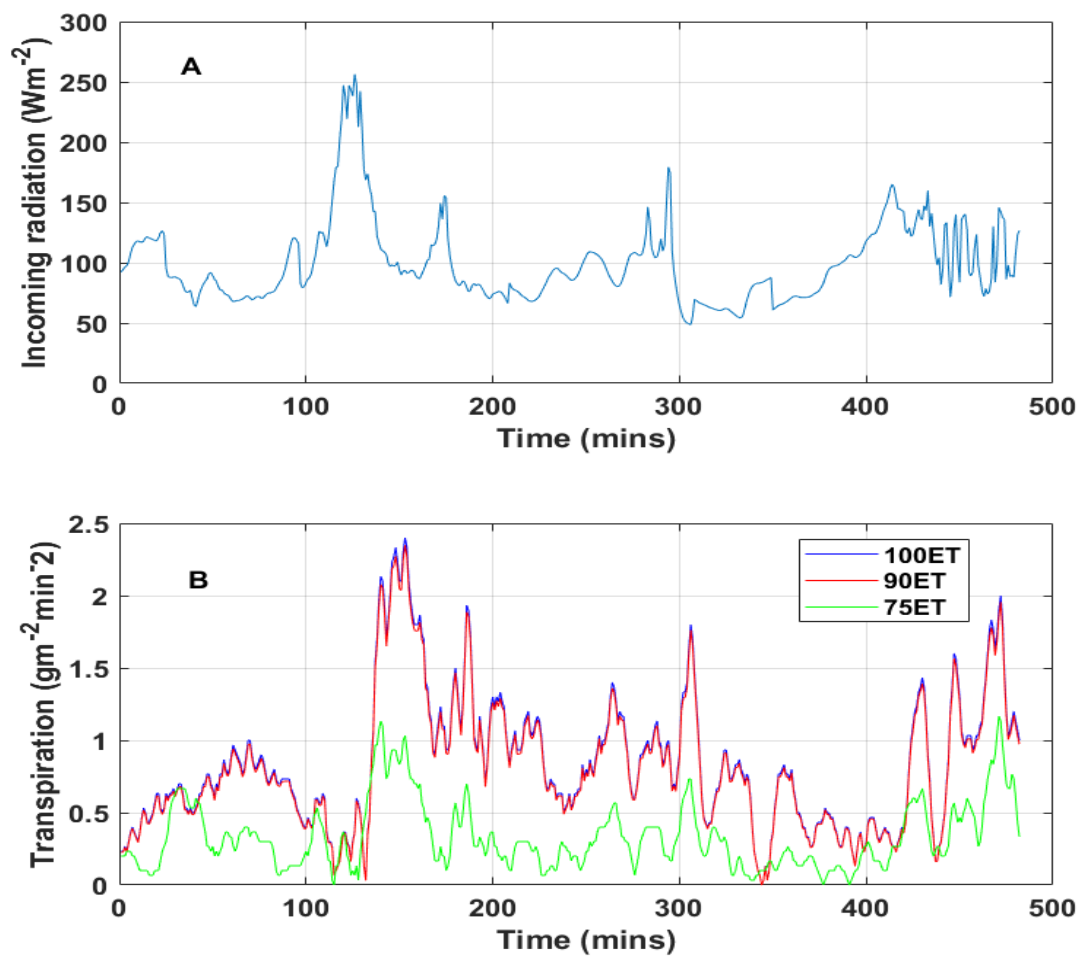
301 The nighttime transpiration of the plants was negligible all through the study period, with a  
302 maximum cumulative transpiration of 3 g being recorded. As such, the daytime transpiration  
303 recorded between 8:00 am and 4:00 pm was further explored.

### 304 **4.1 Dynamics of crop transpiration**

305 The measured typical daily dynamics of the crop transpiration along with prevailing  
306 environmental conditions for a sunny and cloudy day are presented in Figure 2 and Figure 3  
307 respectively. It is seen that the 100ET and 90ET plants maintain a higher transpiration rate  
308 when compared to the 75ET plants. The transpiration dynamics also seem to follow the  
309 dynamics of the incoming radiation. However, there isn't a significant difference in the  
310 transpiration rates of the 100ET and 90ET plants ( $p > 0.1$ ). Stomatal conductance  
311 measurements conducted on the plants also didn't indicate a significant difference in their  
312 water status ( $p > 0.1$ ). The reverse was the case for comparisons of stomatal conductance  
313 measurements of both the 100ET and 90ET plants with the 75ET plants. In Figure 2 and  
314 Figure 3, the datapoints indicating a higher transpiration rate for the 75ET plants are  
315 attributed to measurement errors. This anomaly is addressed in section 4.2.

316 Overall, the difference in transpiration rate between both the 100ET and 90ET plants, and  
317 the 75ET plants indicated a significant difference in their plant water status. This is in  
318 agreement with the results presented by Agam et al. (2013). They reported a significant  
319 difference in the transpiration rates of well-watered and water-stressed olive trees. During  
320 the course of the study, a maximum transpiration rate of  $1.8 \text{ gm}^{-2}\text{min}^{-1}$  was recorded for  
321 the 75ET plants while a value of  $3.2 \text{ gm}^{-2}\text{min}^{-1}$  was recorded for the 90ET and 100ET  
322 plants.

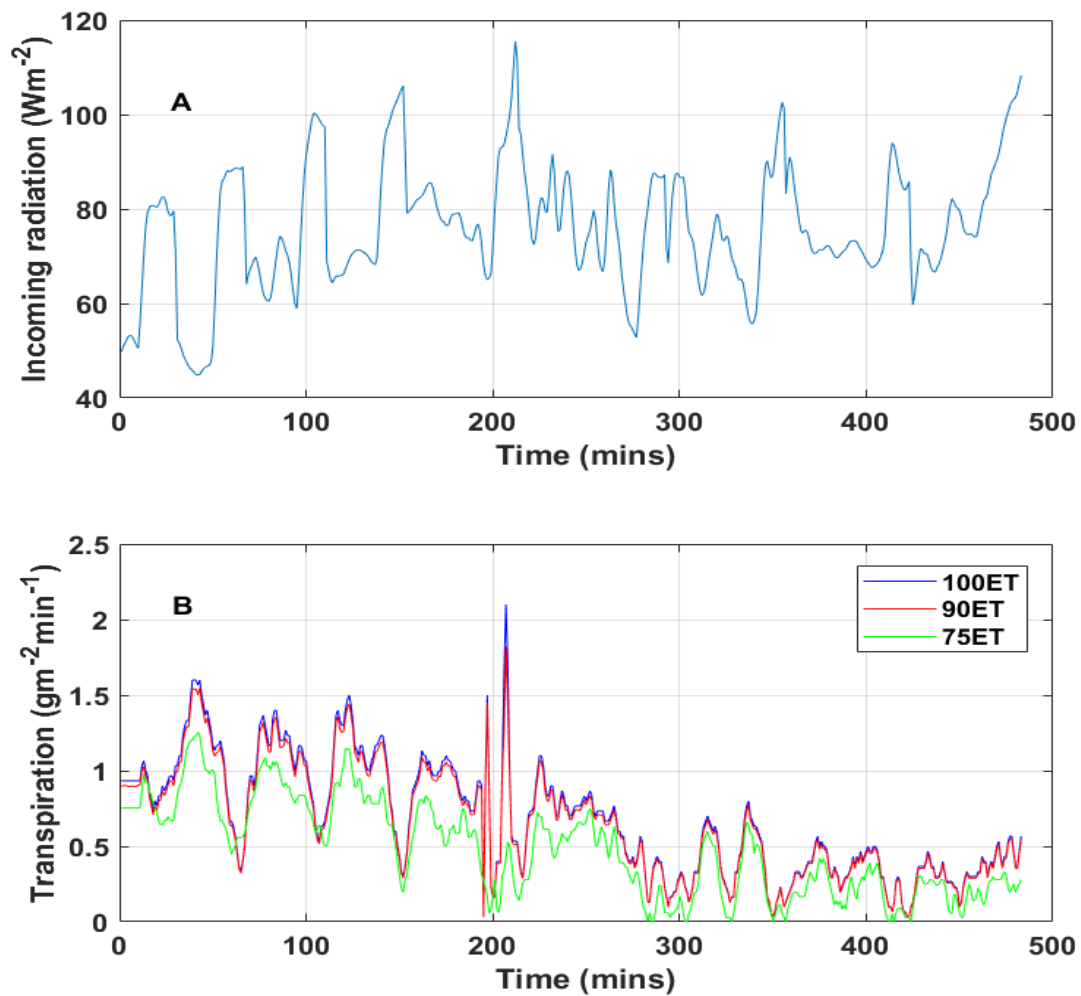
323 Due to the non-significant difference in the transpiration and water status of the 100ET and  
324 90ET plants, the 100ET and 75ET plants were considered in the subsequent analysis.



325

326 Figure 2: Measured incoming radiation and transpiration dynamics of the lettuce crops

327 during a sunny day (a) incoming radiation (b) transpiration



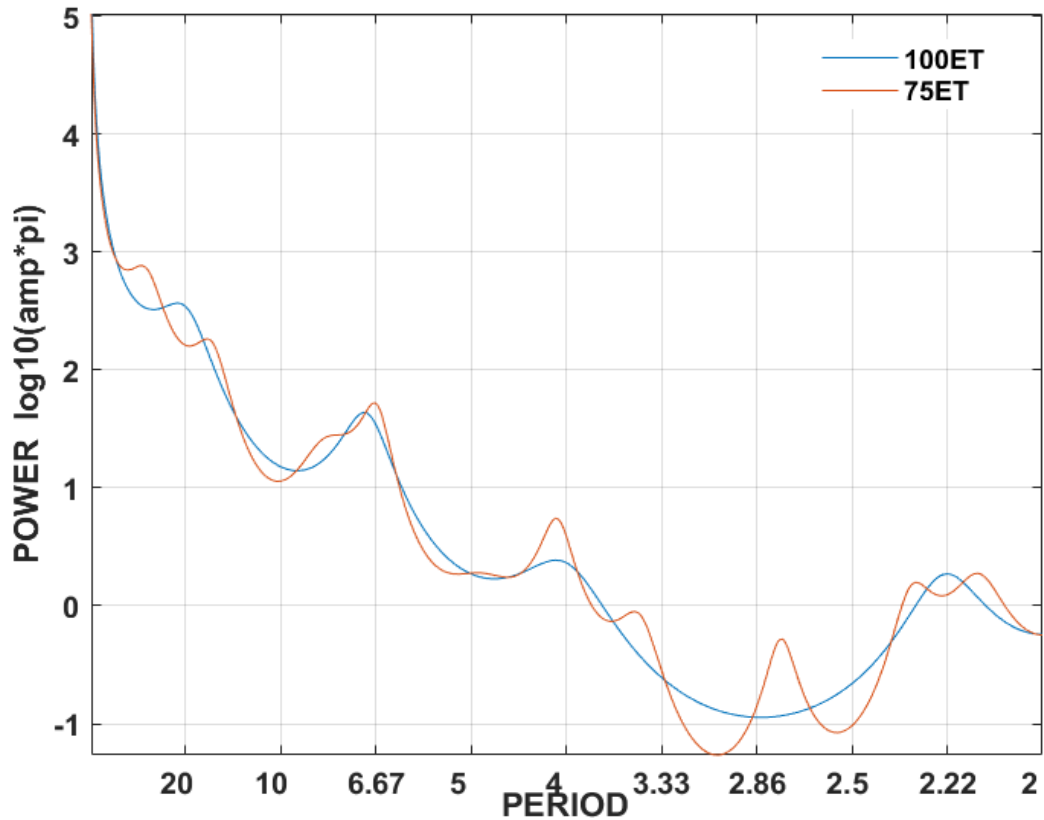
328

329 Figure 3: Measured incoming radiation and transpiration dynamics of the lettuce plants  
 330 during a cloudy day (a) incoming radiation (b) transpiration

331 **4.2 Decoupling and filtering of the transpiration signals**

332 The measured transpiration signals contained different components, some of which were of  
 333 low amplitude and others characterized by higher amplitudes. The higher amplitude  
 334 components were determined to be a result of measurement noise and short-term variability  
 335 in the environment. Such components were decoupled and analysed by calculating the  
 336 power spectrum of the measured signals using fast Fourier transformation algorithm (FFT)  
 337 (Welch, 1967). Figure 4 shows an example of the power spectrum results obtained from the

338 measured transpiration signals. The results showed that the signals are a combination of  
 339 different components that have statistical characteristics but which cannot be observed  
 340 directly (Taylor et al., 2007).



341

342 Figure 4: Power spectrum of the measured transpiration signals

343 The overall transpiration signal  $T_p(t)$  as a function of the different components can be  
 344 represented by the following discrete time equation

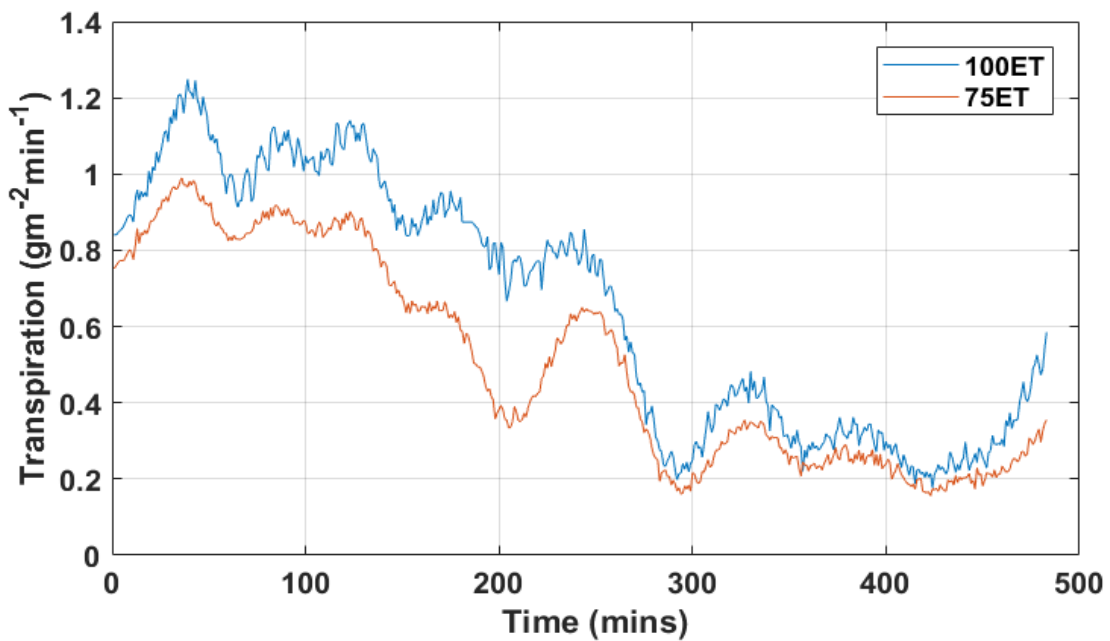
$$345 \quad T_p(t) = T_k + C_k + f_{(uk)} + e_k \quad (5)$$

346 Where  $T_k$  is the trend or low frequency component,  $C_k$  is the cyclical or higher frequency  
 347 component,  $f_{(uk)}$  captures the influence of the input variables and  $e_k$  is the noise  
 348 component.

349 To reduce model complexity, only the  $T_k$  and  $f_{(uk)}$  components of the transpiration signal  
350 were considered. The components are decoupled from the measured transpiration signals  
351 and represented as

$$352 \quad y(k) = T_k + f_{(uk)} \quad (6)$$

353 Where  $y(k)$  is the decoupled transpiration signal. As an example, the decoupled  
354 transpiration signals of the 100ET and 75ET plants shown in Figure 3 are presented in  
355 Figure 5. It can be seen that their transpiration dynamics is clearly separated and the  
356 measurement noise is sufficiently filtered.



357

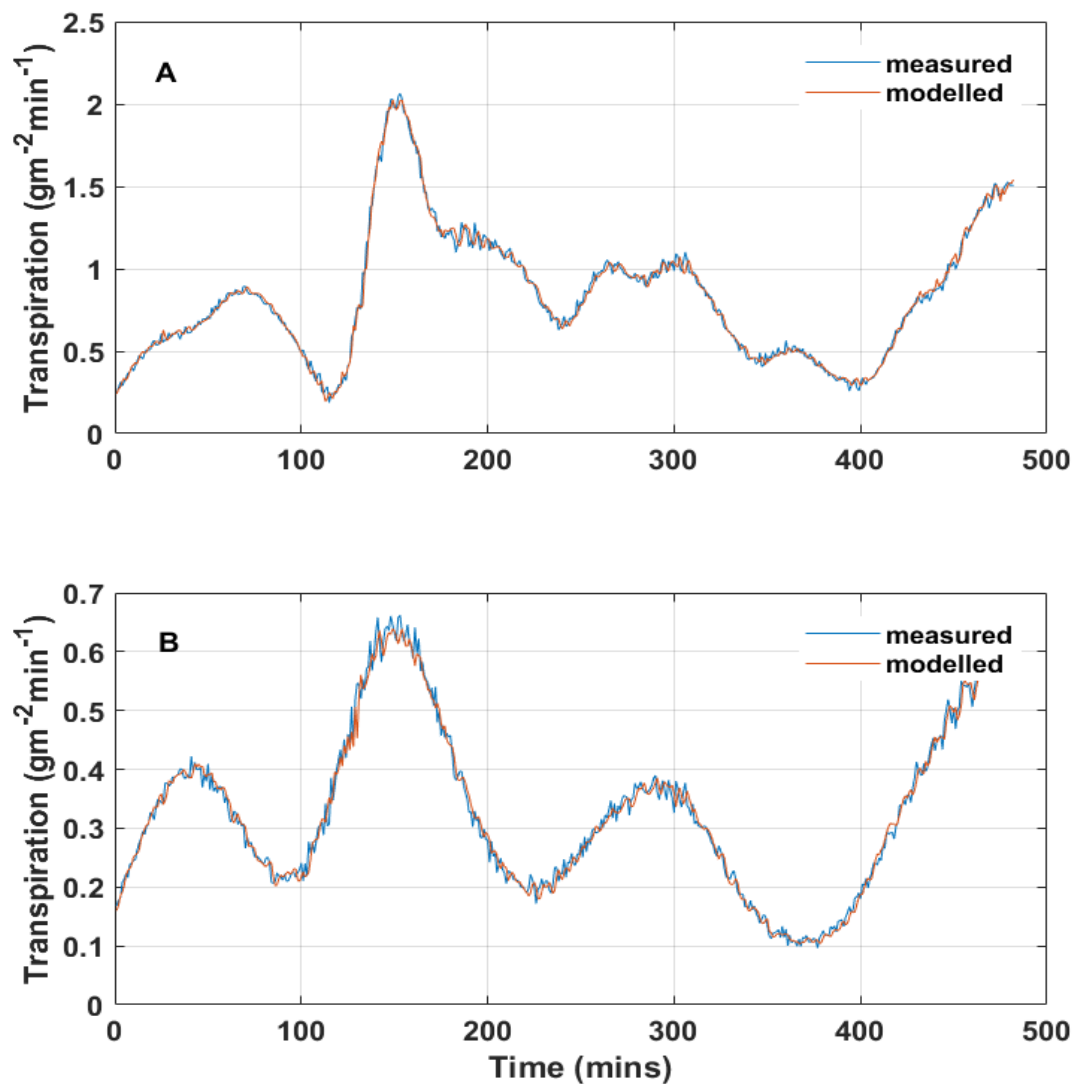
358 Figure 5: Decoupled transpiration signals

### 359 **4.3 System Identification and dynamic modelling of the plant transpiration**

360 The dynamic model of the plant transpiration was identified online by applying system  
361 identification on the incoming time-series data of the measured transpiration rate and  
362 environmental variables.

363 A second-order discrete-time transfer function model was sufficient to describe the  
364 transpiration dynamics with an average coefficient of determination  $R_T^2 = 0.93 \pm 0.04$  and  
365 average Young identification criterion  $YIC = -8.00 \pm 3.00$  (Young and Jakeman, 1980).

366 An example of the measured and modelled transpiration rate for the 100ET and 75ET plants  
367 is presented in Figure 6. It is seen that the modelled values closely match that measured  
368 values while capturing the dominant dynamics.



369

370 Figure 6: Measured and modelled transpiration dynamics of the lettuce plants (a) 100ET (b)

371 75ET

372 The time delay associated with the input parameters was however found to vary as a  
 373 function of plant growth. As such, the LAI was used to divide the model into different  
 374 intervals as summarized in Table 1. For the division, it is easy to change the LAI into other  
 375 time units such as days after planting.

376 Table 1 – Results of the model identification as a function of the LAI interval.  $n$  is the  
 377 equation's order,  $m_{SR}$  is the number of parameters associated with the radiation input,  $m_{VPD}$   
 378 is the number of parameters associated with the VPD input.  $\delta_{SR}$  and  $\delta_{VPD}$  are the time delay  
 379 associated with the radiation and VPD inputs respectively.

LAI interval	$n$	$m_{SR}$	$m_{VPD}$	$\delta_{SR}$	$\delta_{VPD}$
0.8 or lower	2	2	2	0	0
0.8 to 1.6	2	2	2	2	0
1.6 or higher	2	2	2	4	0

380 Sánchez et al. (2012) reported that a dynamic model of the transpiration is able to overcome  
 381 the limitations encountered by steady-state models of crop transpiration. These include the  
 382 overestimation of transpiration rates at low values of LAI and underestimation at higher  
 383 values. The steady-state models are also unable to sufficiently capture the dominant  
 384 dynamics which results in an advancement of the real dynamics over the modelled values.

385 **4.4 Online update of model parameters and prediction of the plant transpiration rate**

386 The biosystem, such as the lettuce plant, is a complex assemblage of interacting physical,  
 387 chemical and biological processes. As such, its transpiration dynamics will vary from day to  
 388 day due to changes in the stomatal response, biological adaptation, and the prevailing  
 389 environment. Accordingly, during the follow-up study, the parameters of the identified  
 390 models were updated at the start of each diurnal measurement period.

391 It was found that the incoming time-series measurements of input/output data obtained  
 392 during the first 120 mins of active transpiration were sufficient to model the transpiration  
 393 dynamics of the plants in a defined water status state. The parameterized model was then  
 394 applied in predicting the transpiration dynamics for the subsequent time period and updated  
 395 after 240 mins. Explained further, at the start of active transpiration at time  $t - 120$ , the data  
 396 points recorded during the time period  $t - 120$  to  $t$  were used for parameter identification  
 397 and prediction was made during time  $t$  to  $t + 240$ . At time  $t + 240$ , the model parameters  
 398 were then updated recursively using data points recorded during  $t$  to  $t + 240$  which were  
 399 flagged as conforming to the defined water status state. Predictions are then made for the  
 400 subsequent time period.

401 The average prediction performance of the model is summarized in Table 2. Table 2 shows  
 402 that the models are able to achieve a satisfactory level of performance at all crop growth  
 403 stages

404 Table 2 – Average prediction performance of the identified models. Standard deviations are  
 405 included in the brackets

LAI interval	Mean absolute error( $gm^{-2}min^{-1}$ )	Root mean square error ( $gm^{-2}min^{-1}$ )
0.8 or lower	0.05 ( $\pm 0.0035$ )	0.06 ( $\pm 0.0044$ )
0.8 to 1.6	0.13 ( $\pm 0.0106$ )	0.15 ( $\pm 0.0128$ )
1.6 or higher	0.09 ( $\pm 0.0046$ )	0.11 ( $\pm 0.0059$ )

406

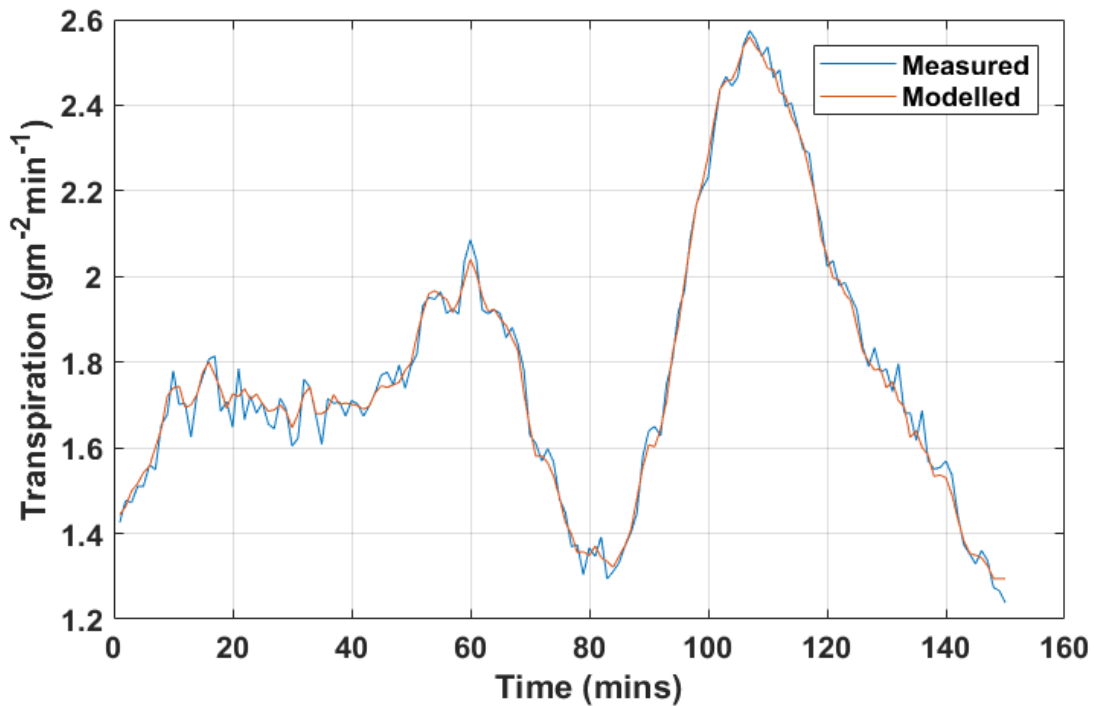
407 Pollet et al. (2000) reported results for a PM type model for estimating the transpiration of  
 408 greenhouse grown lettuce plants. They reported a 6% overestimation of transpiration by the

409 model. It should also be noted that the parameters of PM type models are fitted for a  
410 particular water status state. The dynamic modelling approach presented in the paper can  
411 easily be applied to a plant at any water status state. This is because the parametrization of  
412 the model can be achieved using routinely measured environmental variables and  
413 transpiration measurements. The need to explicitly model the stomatal response is  
414 eliminated as this is implicitly accounted for in the online estimated model parameters and  
415 time delay. This is in agreement with the conclusions of Sánchez et al. (2012).

#### 416 ***4.5 Monitoring of plant water status***

417 The transpiration rate of lettuce plants is dependent on their water status as demonstrated in  
418 section 4.1. This suggests that the difference in the transpiration dynamics as a function of  
419 water status can be exploited as a means of monitoring the water status of the plants.

420 As an example, in Figure 7, the model predicted transpiration dynamics of lettuce plants for  
421 which irrigation was not withheld along with the measured values during a measurement  
422 period is shown. It should be noted that data points applied in parameter identification are  
423 not included in the prediction phase. The measured and modelled values closely match each  
424 other during this period as irrigation was not withheld from the plants; this period of normal  
425 irrigation is defined as state 1. Succinctly, parameter identification was conducted in state 1  
426 and prediction was made at a later period when the plants remained in state 1. The average  
427 stomatal conductance recorded for the plants during this period was  $139.22(\pm 1.14)$   
428  $mmolm^{-2}s^{-1}$  and the average soil moisture content was  $0.18(\pm 0.002) m^3m^{-3}$ , a value close  
429 to the field capacity of the growing media.



430

431 Figure 7: Measured and model predicted transpiration dynamics during a period of normal  
 432 irrigation

433 Figure 8 shows the measured and model predicted transpiration dynamics of the set of  
 434 plants for which irrigation was withheld after a period of normal irrigation, defined as state 2.

435 It is seen that there is a wide deviation between the measured and model predicted values.

436 This is because the model was parameterized for a water status state of the plant during

437 which irrigation was constantly applied to replace transpiration water loss (state 1). The

438 average stomatal conductance recorded during this period was  $116.94(\pm 0.92) \text{ mmolm}^{-2}\text{s}^{-1}$

439 while the average soil moisture content was  $0.16(\pm 0.001) \text{ m}^3\text{m}^{-3}$ . The stomatal

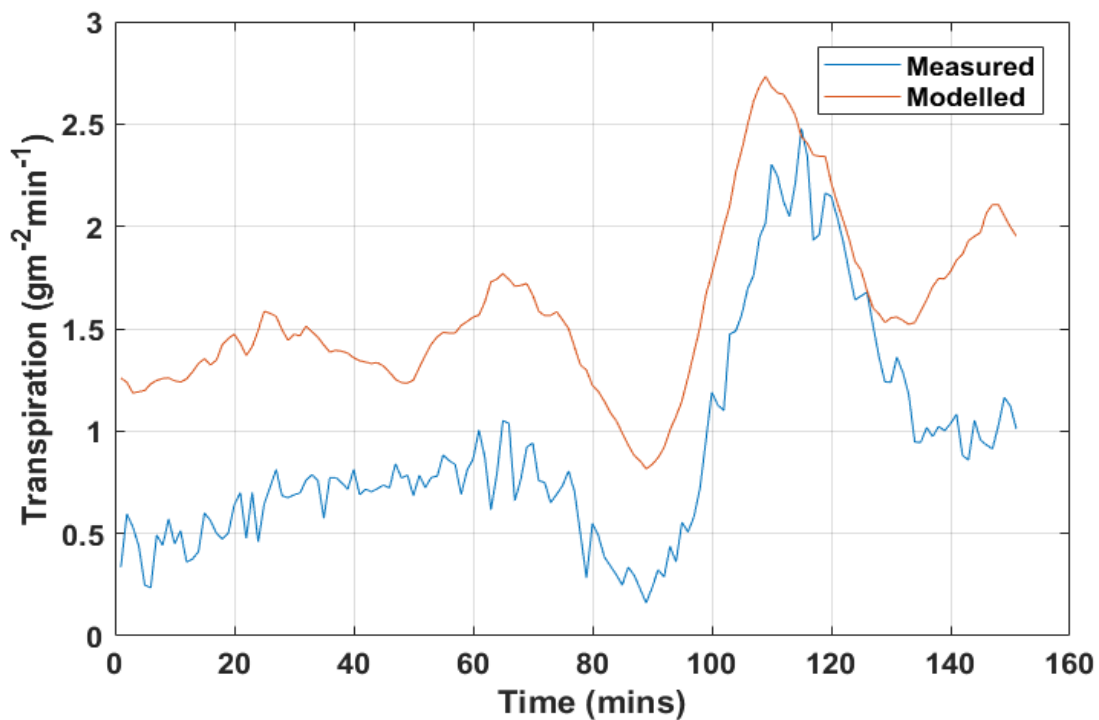
440 conductance values show a clear significant difference ( $p < 0.05$ ) in water status of the

441 plants in state 1 and state 2. It is interesting to note that this difference in plant water status

442 is also indicated in the measured transpiration rate even though the soil moisture status was

443 above the maximum allowable depletion level of 35% (lower soil moisture target = 0.15

444  $\text{m}^3\text{m}^{-3}$ ) defined for the lettuce crop.



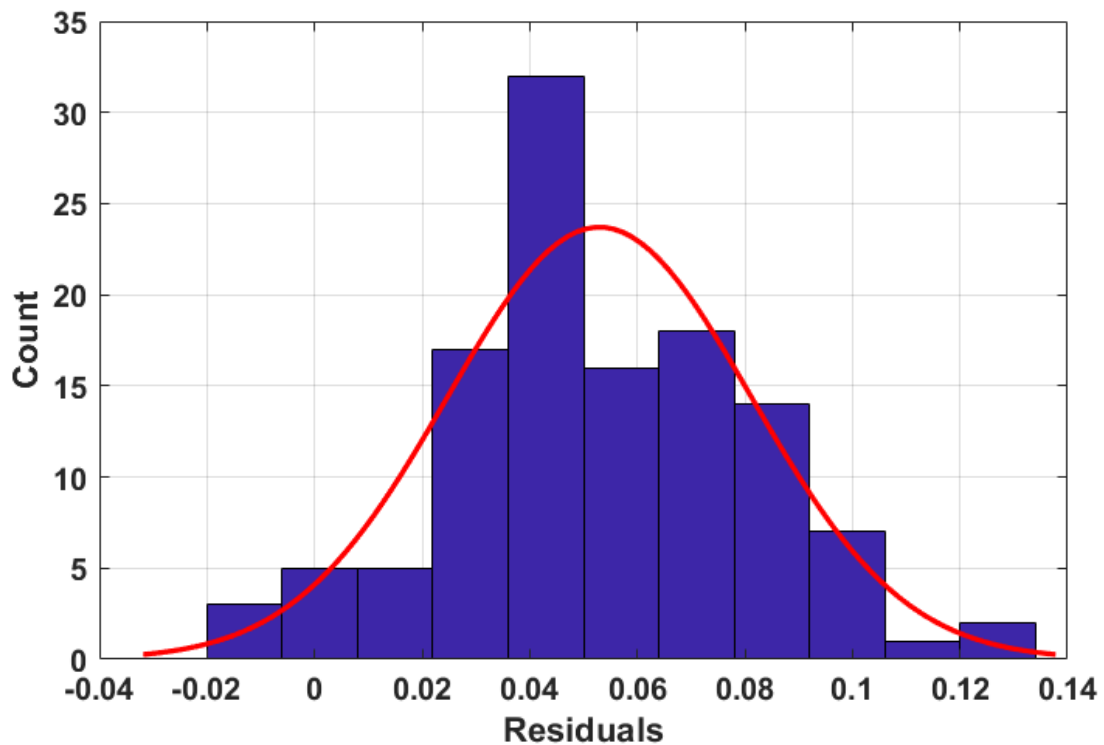
445

446 Figure 8: Measured and model predicted transpiration dynamics during a period after which  
 447 irrigation had been withheld

448 These results give evidence that the transpiration dynamics can indeed be applied as a tool  
 449 for monitoring the water status of the lettuce crop. This was consistently shown in the data  
 450 obtained all through the follow-up study. The results also show that the proposed water  
 451 status monitoring framework is able to exploit the deviation in transpiration dynamics to  
 452 provide information on a change plant water status with a sensitivity similar to stomatal  
 453 conductance measurements.

454 Figure 9 shows the distribution of the residuals during the identification phase in state 1  
 455 (normal irrigation). The residuals conform to a Gaussian distribution suggesting a well-  
 456 defined model for the state.

457 Figure 10 shows the range of the predicted probabilities of observing the data points of the  
 458 residuals in the identification phase in state 1, during prediction in state 1 and during  
 459 prediction in state 2.



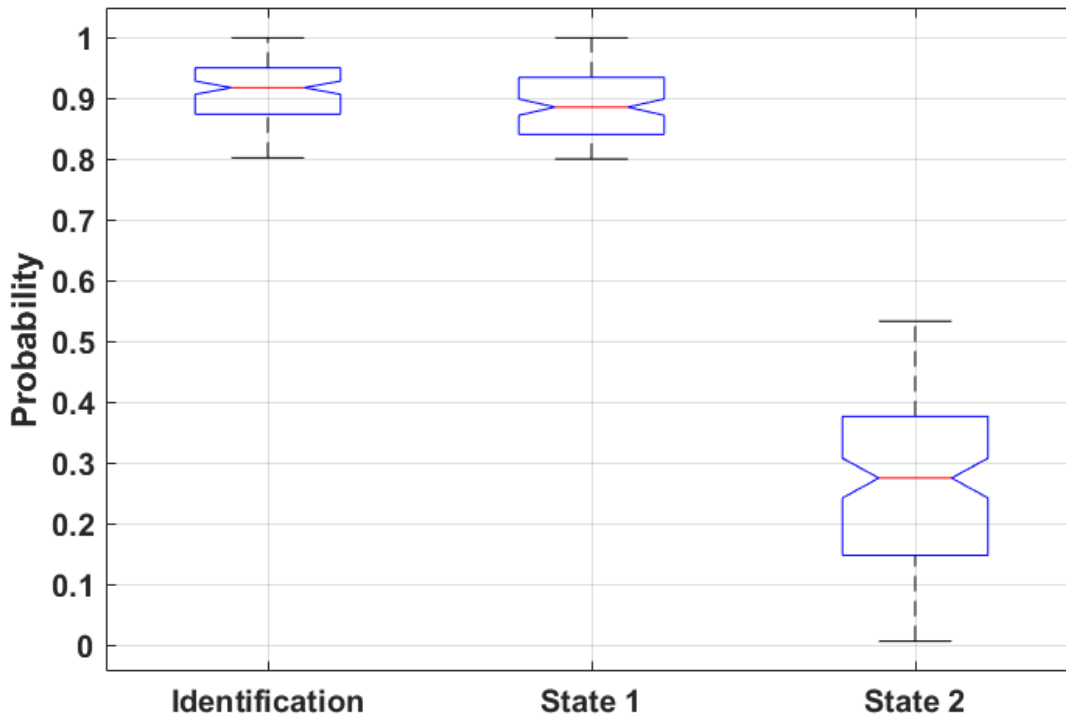
460

461 Figure 9: The distribution of the residuals obtained during the system identification phase

462 These predictions were made using the Gaussian mixture model fitted on the residuals  
 463 obtained during system identification. Figure 10 shows that there is a high probability of  
 464 observing the data points during the identification phase and also during prediction in the  
 465 state for which the model was identified. The lowest probability of observing the data point of  
 466 the residuals during the prediction in state 1 was 0.8. The reverse was the case during  
 467 predictions in state 2. Low probabilities were predicted for observing the data points of the  
 468 residuals in this state, with the highest probability predicted being 0.53. In Figure 10, the  
 469 notches of the identification and state 1 boxes overlap which indicates that the median of  
 470 their predicted probabilities is not significantly different at 5% significance level. It can also  
 471 be seen that notches of the state 2 box do not overlap with the two other boxes indicating a  
 472 significant difference in its median value when compared with the other predicted  
 473 probabilities. The information contained in the predicted probabilities of observing the data  
 474 points of the residuals provides an adequate indication of the water status state of the plants

475 i.e. high probabilities will be predicted when the plant is in the state for which the model was  
476 identified and low probabilities will be predicted when there is a significant change in the  
477 water status state.

478



479

480 Figure 10: Boxplot of the probabilities predicted by the Gaussian Mixture Model fitted on the  
481 residuals obtained during the system identification phase for the identification residuals,  
482 state 1 residuals and state 2 residuals

483 Previous studies e.g. Earl (2003), Prehn et al. (2010), Beeson (2011) have also attempted to  
484 use the measured transpiration rate as a tool for monitoring the onset of drought/water  
485 stress. They attempt to achieve this by comparing the measured transpiration rate at a  
486 particular instance to the initial transpiration rate of the same plant when in a well-watered  
487 state. They, however, neglect the influence of the prevailing environment on the transpiration  
488 dynamics. The model presented in this paper addresses this drawback by predicting the

489 'healthy state' transpiration rate as a function of the known water status and real-time  
490 measurements of the environmental variables.

491 The water status monitoring tool proposed in this paper can be applied in regulating the  
492 water deficit of greenhouse crops. This can be achieved by applying system identification to  
493 identify a model for the plant transpiration at a known water status state and then comparing  
494 the real-time measurements to the model prediction. This approach is used extensively for  
495 performing fault detection in the process industry (Das et al., 2012; Sharma et al., 2010).

496 The intensity of water deficit can be easily quantified by computing the transpiration ratio  
497 proposed by Fernández et al. (2008). This is defined as the ratio between the actual  
498 transpiration measured on a plant and the transpiration rate expected for a well-watered  
499 plant. A value of 1 will indicate the absence of a deficit and a value of zero will indicate a  
500 severe deficit. This can be adapted to compute a deficit intensity for any desired reference  
501 water status state.

502 It should be noted that the system identification modelling technique constitutes a data-  
503 driven approach in which the dynamic response of the plant transpiration is parametrized for  
504 the specific ranges of environmental and crop conditions encountered during model  
505 development, and therefore the models are only applicable to the specific crop and  
506 environment for which they are developed.

507

## 508 **5 Conclusions**

509 A model for predicting the transpiration dynamics of greenhouse cultivated lettuce plants is  
510 presented in this paper. The data-driven model has the incoming radiation, vapour pressure  
511 deficit as input variables, and its structure varies as a function of plant growth in form of the  
512 LAI evolution.

513 Experimental results indicated that the transpiration dynamics of lettuce plants varied as a  
514 function of their water status. This phenomenon was therefore exploited as a tool for  
515 monitoring the water status of the plants. A model of the plant transpiration is identified  
516 online at a period during which the plant is in a desirable and known water status state. This  
517 model is then applied in predicting the crop transpiration. When there is a significant change  
518 in the water status state, the identified model is unable to explain the measured  
519 transpiration, resulting in a change in the statistical properties of the calculated residuals.

520 This approach has an advantage over similar approaches which use the plant transpiration  
521 as an indicator of its water status because it takes the time-varying nature of the plant  
522 system into account through the online adaptation of the model parameters. The difficult to  
523 model variation in stomatal response is also implicitly accounted during the online parameter  
524 estimation. This makes it a suitable plant water status monitoring tool in commercial  
525 greenhouses where the application of mechanistic models have received limited attention,  
526 due to their complexity and large input requirements. The implementation of this model in a  
527 commercial greenhouse and model development for other high-value crops will be the focus  
528 of future research.

529 **Acknowledgements:** The authors wish to acknowledge John Oldacre foundation for funding  
530 this research project

## 531 **References**

532 Adeyemi, O., Grove, I., Peets, S., Norton, T., 2017. Advanced Monitoring and Management  
533 Systems for Improving Sustainability in Precision Irrigation. *Sustainability* 9, 1–29.

534 <https://doi.org/10.3390/su9030353>

535 Agam, N., Cohen, Y., Berni, J.A.J., Alchanatis, V., Kool, D., Dag, A., Yermiyahu, U., Ben-  
536 Gal, A., 2013. An insight to the performance of crop water stress index for olive trees.

537 *Agric. Water Manag.* 118, 79–86. <https://doi.org/10.1016/j.agwat.2012.12.004>

- 538 Allen, R., Pereira, L.S., Raes, D., Smith, M., 1998. FAO Irrigation and Drainage Paper  
539 No.56, FAO. <https://doi.org/10.1016/j.eja.2010.12.001>
- 540 Baille, M., Baille, A., Laury, J.C., 1994. A simplified model for predicting evapotranspiration  
541 rate of nine ornamental species vs. climate factors and leaf area. *Sci. Hortic.*  
542 (Amsterdam). 59, 217–232. [https://doi.org/10.1016/0304-4238\(94\)90015-9](https://doi.org/10.1016/0304-4238(94)90015-9)
- 543 Baptista, F.J., Meneses, J.F., Bailey, B.J., 2005. Measuring and modelling transpiration  
544 versus evapotranspiration of a tomato crop grown on soil in a mediterranean  
545 greenhouse. *Acta Hortic.* 691, 313–320.
- 546 Barnard, D.M., Bauerle, W.L., 2015. Species-specific irrigation scheduling with a spatially  
547 explicit biophysical model: A comparison to substrate moisture sensing with insight into  
548 simplified physiological parameterization. *Agric. For. Meteorol.* 214–215, 48–59.  
549 <https://doi.org/10.1016/j.agrformet.2015.08.244>
- 550 Beeson, R.C., 2011. Weighing lysimeter systems for quantifying water use and studies of  
551 controlled water stress for crops grown in low bulk density substrates. *Agric. Water*  
552 *Manag.* 98, 967–976. <https://doi.org/10.1016/j.agwat.2011.01.005>
- 553 Ben-Gal, A., Agam, N., Alchanatis, V., Cohen, Y., Yermiyahu, U., Zipori, I., Presnov, E.,  
554 Sprintsin, M., Dag, A., 2009. Evaluating water stress in irrigated olives: Correlation of  
555 soil water status, tree water status, and thermal imagery. *Irrig. Sci.* 27, 367–376.  
556 <https://doi.org/10.1007/s00271-009-0150-7>
- 557 Ben-Gal, A., Kool, D., Agam, N., van Halsema, G.E., Yermiyahu, U., Yafe, A., Presnov, E.,  
558 Erel, R., Majdop, A., Zipori, I., Segal, E., Rüger, S., Zimmermann, U., Cohen, Y.,  
559 Alchanatis, V., Dag, A., 2010. Whole-tree water balance and indicators for short-term  
560 drought stress in non-bearing “Barnea” olives. *Agric. Water Manag.* 98, 124–133.  
561 <https://doi.org/10.1016/j.agwat.2010.08.008>

562 Bennis, N., Duplaix, J., Enéa, G., Haloua, M., Youlal, H., 2008. Greenhouse climate  
563 modelling and robust control. *Comput. Electron. Agric.* 61, 96–107.  
564 <https://doi.org/10.1016/j.compag.2007.09.014>

565 Blonquist, J.M., Norman, J.M., Bugbee, B., 2009. Automated measurement of canopy  
566 stomatal conductance based on infrared temperature. *Agric. For. Meteorol.* 149, 2183–  
567 2197. <https://doi.org/10.1016/j.agrformet.2009.10.003>

568 Boonen, C., Joniaux, O., Janssens, K., Berckmans, D., Lemeur, R., Kharoubi, A., Pien, H.,  
569 2000. Modeling dynamic behavior of leaf temperature at three-dimensional positions to  
570 step variations in air temperature and light. *Trans. ASAE-American Soc. Agric. Eng.* 43,  
571 1755–1766. <https://doi.org/10.13031/2013.3078>

572 Chen, B.S.E., Chang, Y.T., 2008. A review of system identification in control engineering,  
573 signal processing, communication and systems biology. *J Biomechatronics Eng* 1, 87–  
574 109.

575 Daniel, C., Schmidt, S., Adriano, F., Pereira, D.C., Oliveira, A.S. De, Fonseca, J., Júnior, G.,  
576 Vellame, L.M., 2013. Design , installation and calibration of a weighing lysimeter for  
577 crop evapotranspiration studies para estudos de evapotranspiração de culturas  
578 agrícolas 77–85.

579 Das, A., Maiti, J., Banerjee, R.N., 2012. Process monitoring and fault detection strategies: a  
580 review. *Int. J. Qual. Reliab. Manag.* 29, 720–752.  
581 <https://doi.org/10.1108/02656711211258508>

582 Davis, S.L., Dukes, M.D., 2010. Irrigation scheduling performance by evapotranspiration-  
583 based controllers. *Agric. Water Manag.* 98, 19–28.  
584 <https://doi.org/10.1016/j.agwat.2010.07.006>

585 Delgoda, D., Malano, H., Saleem, S.K., Halgamuge, M.N., 2016. Irrigation control based on

586 model predictive control (MPC): Formulation of theory and validation using weather  
587 forecast data and AQUACROP model. *Environ. Model. Softw.* 78, 40–53.  
588 <https://doi.org/10.1016/j.envsoft.2015.12.012>

589 Earl, H.J., 2003. A Precise Gravimetric Method for Simulating Drought Stress in Pot  
590 Experiments. *Crop Sci.* 43, 1868–1873. <https://doi.org/10.2135/cropsci2003.1868>

591 Fatnassi, H., Boulard, T., Lagier, J., 2004. Simple indirect estimation of ventilation and crop  
592 transpiration rates in a greenhouse. *Biosyst. Eng.* 88, 467–478.  
593 <https://doi.org/10.1016/j.biosystemseng.2004.05.003>

594 Fernández, J.E., Green, S.R., Caspari, H.W., Diaz-Espejo, A., Cuevas, M. V., 2008. The use  
595 of sap flow measurements for scheduling irrigation in olive, apple and Asian pear trees  
596 and in grapevines. *Plant Soil* 305, 91–104. <https://doi.org/10.1007/s11104-007-9348-8>

597 Gil, P., Santos, F., Palma, L., Cardoso, A., 2015. Recursive subspace system identification  
598 for parametric fault detection in nonlinear systems. *Appl. Soft Comput. J.* 37, 444–455.  
599 <https://doi.org/10.1016/j.asoc.2015.08.036>

600 Howell, T., Evett, S., 2004. The Penman-Monteith Method, USDA-Agricultural Research  
601 Service Conservation & Production Research Laboratory.

602 Jolliet, O., Bailey, B.J., 1992. The effect of climate on tomato transpiration in greenhouses:  
603 measurements and models comparison. *Agric. For. Meteorol.* 58, 43–62.  
604 [https://doi.org/10.1016/0168-1923\(92\)90110-P](https://doi.org/10.1016/0168-1923(92)90110-P)

605 Jones, H.G., 2008. Irrigation Scheduling - Comparison of soil, plant and atmosphere  
606 monitoring approaches. *Acta Hortic.* 792, 391–403.

607 Jones, H.G., 2004. Irrigation scheduling: Advantages and pitfalls of plant-based methods. *J.*  
608 *Exp. Bot.* 55, 2427–2436. <https://doi.org/10.1093/jxb/erh213>

609 Kirchsteiger, H., Pölzer, S., Johansson, R., Renard, E., del Re, L., 2011. Direct continuous  
610 time system identification of MISO transfer function models applied to type 1 diabetes.  
611 IEEE Conf. Decis. Control Eur. Control Conf. 5176–5181.  
612 <https://doi.org/10.1109/CDC.2011.6161344>

613 Kochler, M., Kage, H., Stützel, H., 2007. Modelling the effects of soil water limitations on  
614 transpiration and stomatal regulation of cauliflower. *Eur. J. Agron.* 26, 375–383.  
615 <https://doi.org/10.1016/j.eja.2006.12.003>

616 Lozoya, C., Mendoza, C., Aguilar, A., Román, A., Castelló, R., 2016. Sensor-Based Model  
617 Driven Control Strategy for Precision Irrigation. *J. Sensors* 2016.

618 Maes, W.H., Steppe, K., 2012. Estimating evapotranspiration and drought stress with  
619 ground-based thermal remote sensing in agriculture: a review. *J. Exp. Bot.* 63, 695–  
620 709. <https://doi.org/10.1093/jxb/err313>

621 Monteith, J.L., 1973. *Principles of Environmental Physics, Principles of Environmental*  
622 *Physics*. Edward Arnold, London. <https://doi.org/10.1016/B978-0-12-386910-4.00019-6>

623 Montero, J.I., Antón, A., Muñoz, P., Lorenzo, P., 2001. Transpiration from geranium grown  
624 under high temperatures and low humidities in greenhouses. *Agric. For. Meteorol.* 107,  
625 323–332. [https://doi.org/10.1016/S0168-1923\(01\)00215-5](https://doi.org/10.1016/S0168-1923(01)00215-5)

626 Navarro-Hellín, H., Martínez-del-Rincon, J., Domingo-Miguel, R., Soto-Valles, F., Torres-  
627 Sánchez, R., 2016. A decision support system for managing irrigation in agriculture.  
628 *Comput. Electron. Agric.* 124, 121–131. <https://doi.org/10.1016/j.compag.2016.04.003>

629 Pollet, S., Bleyaert, P., Lemeur, R., 2000. Application of the Penman-Monteith model to  
630 calculate the evapotranspiration of head lettuce (*Lactuca sativa* L. var. *capitata*) in  
631 glasshouse conditions. *Acta Hortic.* 519, 151–161.  
632 <https://doi.org/10.17660/ActaHortic.2000.519.15>

633 Prehn, A., Owen, J., Warren, S., Bilderback, T., Albano, J.P., dammeri Schneid, C.C., 2010.  
634 Comparison of Water Management in Container-Grown Nursery Crops using Leaching  
635 Fraction or Weight-Based On Demand Irrigation Control 1 28, 117–123.

636 Quanten, S., De Valck, E., Cluydts, R., Aerts, J.M., Berckmans, D., 2006. Individualized and  
637 time-variant model for the functional link between thermoregulation and sleep onset. *J.*  
638 *Sleep Res.* 15, 183–198. <https://doi.org/10.1111/j.1365-2869.2006.00519.x>

639 Reynolds, D., 2015. Gaussian Mixture Models. *Encycl. Biometrics.*  
640 [https://doi.org/10.1007/978-1-4899-7488-4\\_196](https://doi.org/10.1007/978-1-4899-7488-4_196)

641 Sánchez, J.A., Rodríguez, F., Guzmán, J.L., Arahál, M.R., 2012. Virtual sensors for  
642 designing irrigation controllers in greenhouses. *Sensors* 12, 15244–15266.  
643 <https://doi.org/10.3390/s121115244>

644 Sharma, A.B., Golubchik, L., Govindan, R., 2010. Sensor Faults : Detection Methods and  
645 Prevalence in Real-World Datasets. *ACM Trans. Sens. Networks* 6, 23.  
646 <https://doi.org/10.1145/1754414.1754419>

647 Speetjens, S.L., Stigter, J.D., van Straten, G., 2009. Towards an adaptive model for  
648 greenhouse control. *Comput. Electron. Agric.* 67, 1–8.  
649 <https://doi.org/10.1016/j.compag.2009.01.012>

650 Taylor, C.J., Pedregal, D.J., Young, P.C., Tych, W., 2007. Environmental time series  
651 analysis and forecasting with the Captain toolbox. *Environ. Model. Softw.* 22, 797–814.  
652 <https://doi.org/10.1016/j.envsoft.2006.03.002>

653 Villarreal-Guerrero, F., Kacira, M., Fitz-Rodríguez, E., Kubota, C., Giacomelli, G.A., Linker,  
654 R., Arbel, A., 2012. Comparison of three evapotranspiration models for a greenhouse  
655 cooling strategy with natural ventilation and variable high pressure fogging. *Sci. Hortic.*  
656 (Amsterdam). 134, 210–221. <https://doi.org/10.1016/j.scienta.2011.10.016>

- 657 Welch, P., 1967. The use of fast Fourier transform for the estimation of power spectra: A  
658 method based on time averaging over short, modified periodograms. *IEEE Trans. Audio*  
659 *Electroacoust.* 15, 70–73. <https://doi.org/10.1109/TAU.1967.1161901>
- 660 Xiao, J., Xu, Q., Wu, C., Gao, Y., Hua, T., Xu, C., 2016. Performance evaluation of missing-  
661 value imputation clustering based on a multivariate Gaussian mixture model. *PLoS One*  
662 11, 1–15. <https://doi.org/10.1371/journal.pone.0161112>
- 663 Yan, H.-C., Zhou, J.-H., Pang, C.K., 2017. Gaussian Mixture Model Using Semisupervised  
664 Learning for Probabilistic Fault Diagnosis Under New Data Categories. *IEEE Trans.*  
665 *Instrum. Meas.* 66, 1–11. <https://doi.org/10.1109/TIM.2017.2654552>
- 666 Young, P., Jakeman, A., 1980. Refined instrumental variable methods of recursive time-  
667 series analysis Part III. Extensions. *Int. J. Control* 31, 741–764.  
668 <https://doi.org/10.1080/00207178008961080>
- 669 Young, P.C., 2006. The data-based mechanistic approach to the modelling, forecasting and  
670 control of environmental systems. *Annu. Rev. Control* 30, 169–182.  
671 <https://doi.org/10.1016/j.arcontrol.2006.05.002>
- 672 Young, P.C., Taylor, C.J., Pedregal, D.J., 2007. *The Captain Toolbox*.

673

674

675